PHYSICAL REVIEW B VOLUME 39, NUMBER 8 15 MARCH 1989-I

Excitonic transitions in strained-layer $In_xGa_{1-x}As/InP$ quantum wells

D. Gershoni, H. Temkin, M. B. Panish, and R. A. Hamm
AT&T Bell Laboratories, Murray Hill, New Jersey 07974
(Received 31 October 1988)

A study of the excitonic transitions in pseudomorphic quantum wells of $In_xGa_{1-x}As$ grown intentionally non-lattice-matched on InP is presented. Photoluminescence and photocurrent excitation techniques were employed to monitor the optical transition energies. A model based on phenomenological deformation-potential theory, which includes nonlinear strain, band nonparabolicity, and strain-induced valence-band mixing terms, is used to calculate the optical transition energies. Good agreement with the experimental data over a wide range of strain is obtained for the first time.

Strained-layer superlattices (SLS's) have recently been the subject of great interest in both theory[1-6] and experiments.[6-12] SLS structures of $In_xGa_{1-x}As/InP$ with x ranging from 0 to 1 are an excellent system for this type of study because their strain varies systematically from -3.8% ($x=0$) to $+3.2\%$ ($x=1$). Previously, we used electro-optic techniques[8,11] and admittance spectroscopy[13] to show that most of the change with x in the band-gap discontinuity between InP and $In_xGa_{1-x}As$ layers takes place in the conduction band. A simple phenomenological deformation-potential model has enabled us to calculate the band-offset dependence on In concentration (x) and, in particular, to explain a transition for $x \cong 0.2$ from a type-I to a type-II superlattice.

Here we study the optical transitions between confined particle states of strained-layer quantum wells (SLQW's), using low-temperature photoluminescence (PL), photoluminescence excitation (PLE), and photocurrent excitation (PCE). Well dimensions and compositions were measured by transmission electron microscopy and high-resolution x-ray diffraction (HRXRD). The well-characterized set of samples with excellent optical properties enabled us to compare the observed excitonic transitions with predictions of a model which contains no adjustable parameters. The model includes band nonparabolicity and nonlinear strain effects which we find essential in order to account for the higher-order excitonic transitions observed.

The $In_xGa_{1-x}As/InP$ SLQW samples were grown by gas-source molecular-beam epitaxy (GSMBE)[14] on (100)-oriented InP substrates. The SLQW formed the intrinsic region of a *p-i-n* diode structure. It was grown on a 0.25-μm-thick *n*-type InP buffer layer and consisted of ten periods of strained $In_xGa_{1-x}As$ quantum wells separated by $\sim$400-Å-thick InP barriers. Well widths varied from $\sim$50 to $\sim$100 Å in different samples. The In concentration was varied from $x \cong 0.20$ to $x \cong 0.75$ in order to cover efficiently the type-I superlattice domain.[11] The periodic structure was followed by a 2000-Å-thick unintentionally doped *n*-type InP layer and 3000 Å of *p*-type InP doped to 1×10^{18} cm^{-3}. Well dimensions and the strain component parallel to the growth direction were determined by fitting the satellite pattern in the (4,0,0) HRXRD scans with a kinematic step model simulation described previously.[15]

For the PLE measurements, the as-grown samples were placed in a He-flow cryostat. We have used dispersed light from a tungsten lamp as a continuously tunable source of excitation. The luminescence was monitored by a 0.64-m monochromator followed by a liquid-nitrogen-cooled Ge detector. The spectra were corrected later for the system response. Figure 1 presents the PLE spectra (solid lines) and PL spectra (dashed lines) of five samples. The bars indicate excitonic transition energies calculated with use of the model described below. For the photocurrent response studies, mesa-type photodetectors were prepared. In Fig. 2 we show the room-temperature photocurrent spectra of five samples. The $x=0.73$ sample is not presented in the PLE spectra of Fig. 1 since its luminescence wavelength is hardly detected by the Ge detector. The low-temperature excitonic transitions for

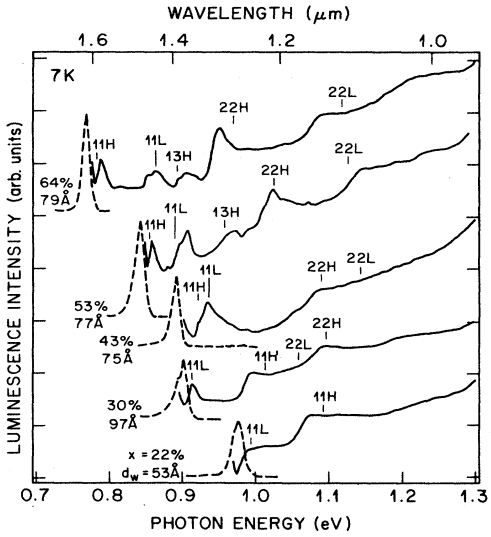

FIG. 1. Low-temperature PL (dashed lines) and PLE (solid lines) spectra of five strained-layer $In_xGa_{1-x}As/InP$ multi-quantum-wells samples. Vertical bars indicate calculated excitonic transitions. The first number above the bar refers to the conduction-band sublevel, the second to the valence-band sublevel, and the letter indicates whether it is a light- (L) or heavy- (H) hole subband.

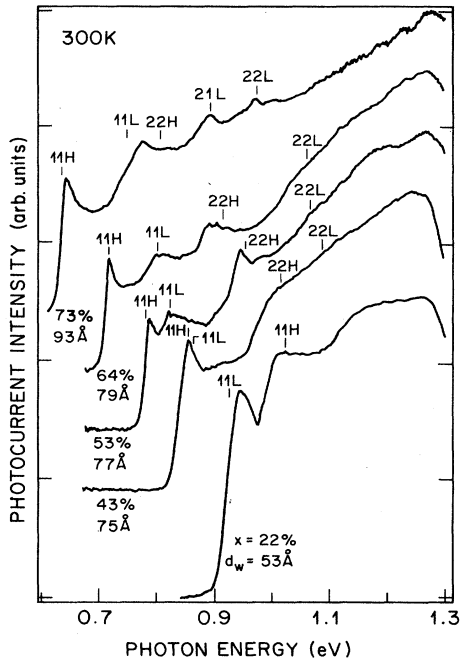

FIG. 2. Room-temperature PCE spectra for five strained-layer $In_xGa_{1-x}As/InP$ multi-quantum-wells samples. Vertical bars indicate calculated excitonic transitions.

this sample were inferred instead from a PCE spectrum which is not shown. Most of the excitonic features are clear even at room temperature. Room-temperature transition energies are marked with vertical bars. These were calculated using the same model, taking into account the temperature dependence of the binaries' band gaps and lattice constants. In general the agreement is good.

Commensurate growth of strained $In_xGa_{1-x}As$ layers on (100)-oriented InP substrate subjects these layers to a biaxial in-plane strain. The epitaxial layers experience a tetragonal distortion, resulting in a very simple form of the strain tensor ϵ_{ij}. Its only nonvanishing components are $\epsilon_{xx}=\epsilon_{yy}=\epsilon_{\parallel}$ and $\epsilon_{zz}=-(2C_{12}/C_{11})\epsilon_{\parallel}=\epsilon_{\perp}$, where $\hat{z}$ was chosen along the growth direction and C_{ij} are the components of the elastic stiffness tensor. Below the critical layer thickness, the in-plane lattice constant of the strained layer is exactly equal to that of the InP substrate. Thus the in-plane strain tensor components are given by

$$\epsilon_{\parallel}=[a_{\mathrm{InP}}-a(x)]/a(x)\,, \tag{1}$$

where a_{InP} is the lattice constant of InP and $a(x)$ is the lattice constant of the relaxed $In_xGa_{1-x}As$. The perpendicular strain component is given by $\epsilon_{\perp}=a_{\perp}/a(x)$, where $a_{\perp}$ is the layer lattice constant in the growth direction. The out-of-plane lattice constant ($a_{\perp}$) is determined directly from the HRXRD, thus providing accurate experimental estimate of x (In concentration) using the above elastic relations, Vegard's law, and the known lattice constants of InAs and GaAs. Linear interpolation procedure is also used to obtain all other material parameters of the ternary alloys, such as the stiffness coefficient tensor components $C_{ij}(x)$ and the strain-free carrier's effective-mass parameters, band and band-gap deformation potentials, and valence-band offsets. All the input parameters are summarized in Table I. Parabolic interpolation, which takes into account the bowing, is used, however, to calculate the strain-free energy-gap dependence on In concentration. Strain effects are introduced now in the following way: The hydrostatic strain contributes to the band-gap change according to

$$\Delta E_g=\{[-dE_g(x)/dp]\tfrac{1}{3}[C_{11}(x)+2C_{12}(x)]\}(2\epsilon_{\parallel}+\epsilon_{\perp})\,, \tag{2}$$

where the expression in the curly brackets is the ternary band-gap hydrostatic deformation potential. In a similar way the conduction-band edge changes its position as $\Delta E_c=a_c(x)(2\epsilon_{\parallel}+\epsilon_{\perp})$, where $a_c(x)$ is the ternary conduction-band hydrostatic deformation potential. The change in valence band is given by $\Delta E_v=\Delta E_g-\Delta E_c$. The nonequal distribution of the hydrostatic-strain-induced change in band gap between the valence bands and conduction bands directly influences the band offsets.[1]

The uniaxial strain introduces two important effects: First, it removes the valence-band degeneracy at the Brillouin-zone center. The splitting between the $J=\frac{3}{2}$, $m_J=\pm\frac{3}{2}$ (heavy hole) valence band and the $J=\frac{3}{2}$, $m_J=\pm\frac{1}{2}$ (light hole) valence band is given by

$$2\epsilon_0=2b_v(x)(\epsilon_{\perp}-\epsilon_{\parallel})\,, \tag{3}$$

where $b_v(x)$ is the ternary valence-band shear deformation potential for the (1,0,0) strain.[16] Second, it mixes the $(\frac{3}{2}\pm\frac{1}{2})$ valence band and the $(\frac{1}{2}\pm\frac{1}{2})$ split-off valence band. This mixing results in another, nonlinear in strain, correction to the valence-band $m_J=\pm\frac{1}{2}$ edges:[16]

$$\Delta E_{\mathrm{NL}}^{\pm}=\pm\tfrac{1}{2}\Delta_0(x)[1+\tfrac{1}{2}X-(1+X+\tfrac{9}{4}X^2)^{1/2}]\,, \tag{4}$$

where the $+$ ($-$) refers to the $\frac{3}{2}\pm\frac{1}{2}$ ($\frac{1}{2}\pm\frac{1}{2}$) valence band. The spin-orbit split-off energy of the unstrained ternary is $\Delta_0(x)$ and $X=\epsilon_0/\Delta_0$. The light-hole band-edge effective mass also needs to be corrected as a result of this mixing:[16]

$$\Delta\left(\frac{1}{m^*_{\mathrm{LH},z}(x)}\right)=\frac{1}{2}\left(\frac{1}{m^*_{\mathrm{LH},z}(x)}-\frac{1}{m^*_{\mathrm{HH},z}(x)}\right)\times\left(\frac{1+9X}{(1+2X+9X^2)^{1/2}}\right). \tag{5}$$

Here $m^*_{\mathrm{HH},z}(x)[m^*_{\mathrm{LH},z}(x)]$ is the heavy- (light-) hole effective mass, in the direction of the growth of the unstrained ternary layer. The corrections introduced by Eqs. (4) and (5) are not very significant for the $n=1$ transitions. They amount to $\sim$20 meV ($\sim$15 meV) for the $x=0.73$ ($x=0.22$) most strained samples in this study.[5] The correction is much more important for higher-order transitions. For example, it amounts to as much as 90 meV for the $n=2$ light-hole excitonic transition in the $x=0.73$ sample.

Taking into account these strain-induced changes in the band-edge energies and effective masses, we now turn to solve the one-dimensional quantum-well problem, with the inclusion of nonparabolicity, for each carrier separately.[17]

TABLE I. Constants used in calculations.

Name	InP	GaAs	InAs	$In_{0.53}Ga_{0.47}As$
E_g (eV)	1.424[a]	1.519[a]	0.418[a]	0.812[b]
Δ_0 (eV)	0.11[a]	0.34[a]	0.37[a]	
m_e^* (emu)	0.079[a]	0.067[a]	0.023[a]	
$m_{LH,z}^*$ (emu)	0.121[c]	0.094[c,d]	0.027[c]	
$m_{HH,z}$ (emu)	0.606[c]	0.341[c,d]	0.4[c]	
Valence-band offset relative to InP (eV)	0	0.34[e]	0.41[e]	
a (Å)	5.8603[f]	5.6416[f]	6.0501[f]	
C_{11} (10^{11} dyn/cm^2)		12.11[a]	8.541[f]	
C_{12} (10^{11} dyn/cm^2)		5.48[a]	4.66[f]	
dE_g/dp(10^{-6} eV cm^2/kg)		11.3[a]	9.8[a]	
a_c (eV)		−7.1[g]	−5.4[g]	
b_v (eV)		−1.7[a]	−1.8[a]	
χ_0		10.9[a]	15.15[a]	
E_B^{LM} (meV)				9[h]

[a] *Semiconductors*, edited by O. Madelung, M. Schulz, and H. Weiss, Landolt-Bornstein, New Series, Group 3, Vol. 17a (Springer-Verlag, Berlin, 1982).
[b] *GaInAsP Alloy Semiconductors*, edited by T. P. Pearsall (Wiley, New York, 1982).
[c] We use $m_{LH,z}^* = 1/(\gamma_1 + 2\gamma_2)$, $m_{HH,z}^* = 1/(\gamma_1 - 2\gamma_2)$, and Luttinger parameters γ_1, γ_2 from footnote a.
[d] D. F. Nelson, R. C. Miller, and D. A. Kleinman, Phys. Rev. B **35**, 1770 (1987).
[e] R. S. Bauer and G. Margaritondo, Phys. Today **40** (No. 1), 27 (1987).
[f] From footnote a, corrected for temperature dependence.
[g] D. L. Camphausen, G. A. Nevill Connel, and W. Paul, Phys. Rev. Lett. **26**, 184 (1971).
[h] Reference 19.

Confined carrier energies were calculated by numerically finding the root of the following equation:

$$f(E) = [r_1(E) - 1/r_1(E)]\sin r_2(E) - 2\cos r_2(E) , \quad (6)$$

where $r_1(E) = K_w(E)m_b^*(E)/K_b(E)m_w^*(E)$ and $r_2(E) = K_w(E)L_w$. L, K, m^* stand for the width, carrier wave vector, and effective mass in the confinement direction. The subscripts w and b denote the well and barrier, respectively. The dispersion relations which correlate the wave vector to the particle energy E are then $E = \hbar^2 K_w^2/2m_w^*(E)$ and $E - V_b = \hbar^2 K_b^2/2m_b^*(E)$, where V_b is the barrier potential or band discontinuity. The effects of band nonparabolicity are introduced through the energy-dependent effective masses of electrons and light holes $m^*(E) = \hbar^2 K^2(E)/2E$, where $K(E)$ is given implicitly by the Kane model dispersion relation[18]

$$E'(E' - E_g)(E' + \Delta) - K^2 P^2 (E' + 2\Delta) = 0 . \quad (7)$$

Here $E' = E + E_i - \hbar^2 K^2/2m_0$, where E_i is the relevant band-edge energy (i.e., E_g for electron), and E_g and Δ are already corrected for strain effects. The free-electron mass is m_0 and P is the $\mathbf{k}\cdot\mathbf{p}$ matrix element, which is chosen so that $m^*(E=0)$ is given by the strain-corrected band-edge effective masses (slightly different P values are obtained, thus, for electron and light hole). In the barriers the energy E is replaced by $E - V_b$, and the same Kane dispersion relation is used. The same procedure was successfully used by us previously in order to account for the nonparabolicity effects on optical transitions in lattice-matched $In_{0.53}Ga_{0.47}As$/InP quantum wells.[19] We have ignored here strain-induced corrections to this procedure.[17] The correction introduced by this procedure can be safely neglected in the case of the lowest $n=1$ transitions. For the $n=2$ heavy- (light-) hole transitions, it is ~10 meV (~60 meV) on the average.[19]

Finally, exciton binding energy is taken into account in the following way:

$$E_B = E_B^{LM}[\mu(x)/\mu^{LM}][\chi_0^{LM}/\chi_0(x)]^2 , \quad (8)$$

where $E_B^{LM} \cong 9$ meV is the exciton binding energy for a

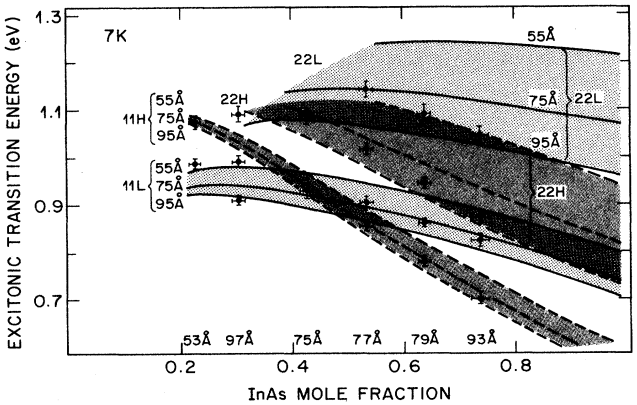

FIG. 3. Calculated allowed ($\Delta n = 0$) excitonic transitions energies, as a function of the InAs mole fraction (x), for 55-, 75-, and 95-Å $In_xGa_{1-x}As$/InP SLQW. The measured energies are also shown (solid circles) for comparison. Bars represent the experimental uncertainties.

lattice-matched quantum well.[19] χ_0 is the dc dielectric constant of the material and μ is the exciton reduced mass:

$$\frac{1}{\mu_\pm} = \frac{1}{m_e^*} + (1 \mp \tfrac{1}{2}) \frac{1}{2m_{\mathrm{HH},z}} + (1 \pm \tfrac{1}{2}) \frac{1}{2m_{\mathrm{LH},z}} . \quad (9)$$

The + (−) sign stands for the heavy- (light-) hole exciton reduced mass. This simple treatment of the excitonic binding energy does not affect the comparison with experiment because the magnitude of this term is at most comparable to the width of the measured spectroscopic transitions. Calculated optical transition energies as a function of In concentration for 55-, 75-, and 95-Å $In_xGa_{1-x}As/InP$ SLQW's are given in Fig. 3 together with the experimental data points extracted from the spectra shown in Fig. 1. The agreement between calculated and measured transitions is good.

Note particularly that the parity-forbidden transition $e2$-LH1 in the $x=0.73$ sample has a much greater oscillator strength than the allowed transition $e2$-HH2. This transition was also observed in nonstrained GaAlAs/GaAs quantum wells of equal dimensions by Miller *et al.*[20] This observation was explained in terms of mixing between light- and heavy-hole states away from the Brillouin-zone center.[21] Our model, which considers only zone-center band edges, cannot take into account such an effect. We believe, however, that strain-induced mixing enhancement between the LH1 and HH2 valence subbands is the reason for the larger oscillator strength of the parity-forbidden excitonic transition in our sample. In the low-temperature PCE spectrum (not shown), both transitions have roughly the same strength. Another forbidden transition (although parity allowed), namely $e1$-HH3, is clearly observed in the PLE spectra of the lattice-matched sample and the $x=0.64$ strained one. This transition, which is also seen in the low-temperature PCE spectrum of the $x=0.73$ sample (not shown), is very well interpreted by the model. Its energy agrees well with calculations and its oscillator strength can be understood in terms of a nonvanishing overlap integral between the carriers envelope wave functions.

In summary, we present a detailed study of the excitonic transitions in pseudomorphic quantum wells of InGaAs/InP. Experimental exciton energies are compared with an effective-mass approximation model, which includes bulk phenomenological deformation potential and elastic theory corrections. The model, which includes nonlinear terms in strain and band nonparabolicity effects, and contains no adjustable parameters, successfully accounts for all the observed optical transitions. In the sample with the highest biaxial compressive strain studied, an enhanced parity-forbidden (light hole 1–electron 2) transition was noticed.

[1] M. Cardona and N. E. Christensen, Phys. Rev. B **35**, 6182 (1987).
[2] R. People, IEEE J. Quantum Electron. **22**, 1696 (1986).
[3] S. Froyen, D. M. Wood, and A. Zunger, Phys. Rev. B **37**, 6893 (1988).
[4] G. D. Sanders and K. K. Bajaj, Phys. Rev. B **35**, 2308 (1987).
[5] L. C. Andreani, A. Pasquarello, and F. Bassani, Phys. Rev. B **36**, 5887 (1987).
[6] S. C. Hong, G. P. Kothiyal, N. Debbar, P. Bhattacharya, and J. Singh, Phys. Rev. B **37**, 878 (1988).
[7] I. J. Fritz, L. R. Dawson, J. J. Drummond, J. E. Schirber, and R. M. Biefeld, Appl. Phys. Lett. **48**, 139 (1986).
[8] D. Gershoni, J. M. Vandenberg, R. A. Hamm, H. Temkin, and M. B. Panish, Phys. Rev. B **36**, 1320 (1987).
[9] C. P. Kuo, S. K. Vong, R. M. Cohen, and G. B. Stringfellow, J. Appl. Phys. **57**, 5428 (1985).
[10] T. G. Anderson, Z. G. Chen, V. D. Kulakovskii, A. Uddin, and J. T. Vallin, Phys. Rev. B **37**, 4032 (1988).
[11] D. Gershoni, H. Temkin, J. M. Vadenberg, S. N. G. Chu, R. A. Hamm, and M. B. Panish, Phys. Rev. Lett. **60**, 448 (1988).
[12] U. Cebulla, G. Trankle, U. Zien, A. Forchel, G. Griffiths, H. Kroemer, and S. Subbana, Phys. Rev. B **37**, 6278 (1988).
[13] R. E. Cavicchi, D. V. Lang, D. Gershoni, A. M. Sergent, J. M. Vandenberg, S. N. G. Chu, and M. B. Panish, Appl. Phys. Lett. (to be published).
[14] M. B. Panish, Prog. Cryst. Growth Charact. **12**, 1 (1986).
[15] J. M. Vandenberg, S. N. G. Chu, R. A. Hamm, M. B. Panish, and H. Temkin, Appl. Phys. Lett. **49**, 1302 (1986).
[16] H. Hasegawa, Phys. Rev. **129**, 1029 (1963).
[17] Note that by doing so, we neglect terms which are common to the crystal momentum (K_z) and to the strain.
[18] E. O. Kane, J. Phys. Chem. Solids **1**, 249 (1957).
[19] D. Gershoni, H. Temkin, and M. B. Panish, Phys. Rev. B **38**, 7870 (1988).
[20] R. C. Miller, A. C. Gossard, G. D. Sanders, Y. C. Chang, and J. N. Schulman, Phys. Rev. B **32**, 8452 (1985).
[21] G. D. Sanders and Y. C. Chang, Phys. Rev. B **32**, 5517 (1985).

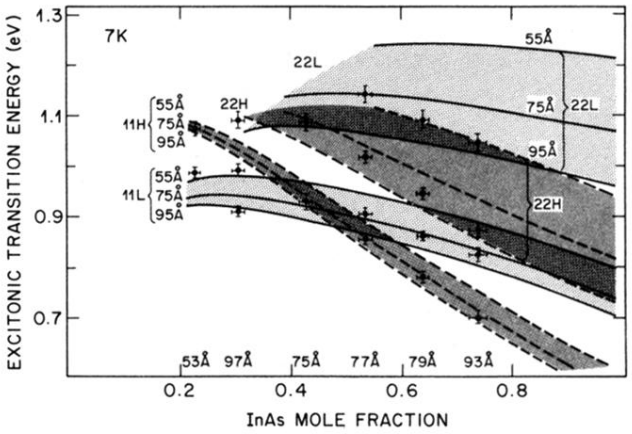

FIG. 3. Calculated allowed ($\Delta n = 0$) excitonic transitions energies, as a function of the InAs mole fraction (x), for 55-, 75-, and 95-Å $In_xGa_{1-x}As/InP$ SLQW. The measured energies are also shown (solid circles) for comparison. Bars represent the experimental uncertainties.